Separation Science and Technology
Publication details, including instructions for authors and subscription information:
http://www.informaworld.com/smpp/title~content=t713708471

The influence of preparation methods and surface properties of activated carbons on Cr(III) adsorption from aqueous solutions

P. Milich[a]; F. Möller[a]; J. Píriz[a]; G. Vivó[a]; N. Tancredi[a]
[a] Laboratorio de Fisicoquímica de Superficies, Departamento de Fisicoquímica, Facultad de Química, Universidad de la República, Montevideo, Uruguay

Online publication date: 11 December 2002

To cite this Article Milich, P. , Möller, F. , Píriz, J. , Vivó, G. and Tancredi, N.(2002) 'The influence of preparation methods and surface properties of activated carbons on Cr(III) adsorption from aqueous solutions', Separation Science and Technology, 37: 6, 1453 — 1467
To link to this Article: DOI: 10.1081/SS-120002621
URL: http://dx.doi.org/10.1081/SS-120002621

SEPARATION SCIENCE AND TECHNOLOGY, 37(6), 1453–1467 (2002)

THE INFLUENCE OF PREPARATION METHODS AND SURFACE PROPERTIES OF ACTIVATED CARBONS ON Cr(III) ADSORPTION FROM AQUEOUS SOLUTIONS

P. Milich, F. Möller, J. Píriz, G. Vivó, and N. Tancredi*

Laboratorio de Fisicoquímica de Superficies, Departamento de Fisicoquímica, Facultad de Química, Universidad de la República, Gral. Flores 2124, CC 1157, 11800, Montevideo, Uruguay

ABSTRACT

Activated carbons were prepared from eucalyptus wood, by using three different "physical" activating methods: air and CO_2 partial gasification of wood char (2 hr, 400°C and 800°C, respectively), and direct CO_2 partial gasification of wood sawdust. The three activated carbons were then oxidized with HNO_3 for increasing the surface concentration of oxygenated functions, and Cr(III) aqueous solution adsorption isotherms were determined for each oxidized carbon. Characterization of the carbons were done through elemental analysis, N_2 adsorption, and Fourier transform infrared spectroscopy spectra. Results show that oxidized activated carbons prepared from air gasification have the higher Cr(III) adsorption capacity. Conclusions about chemical functions

*Corresponding author. E-mail: ntancred@bilbo.edu.uy

formed onto the carbon surface and the relationship with Cr(III) adsorption are exposed.

Key Words: Activated carbon; Porous structure; Nitric acid oxidation; Wood; Chromium (III); Liquid phase adsorption

INTRODUCTION

Activated carbon is an adsorbent with a high carbon content and important interior surface, because of their high pore volume. It is produced from different carbonaceous raw materials, including different kinds of biomass, mostly wood and coconut husk. It is used in gas and liquid purification, including water potabilization and wastewater treatment, solvent recovery, and as a catalyst support (1,2).

Oxidation of activated carbon to increase the surface concentration of acidic oxygenated functions has proved to be a way to improve the adsorption of metallic cations in aqueous solutions (1,3). The pH values, temperature of adsorption, and presence of salts, change the net surface charge of the carbon walls, and the equilibrium among the different water–cations complexes (3–5).

Chromium adsorption onto activated carbons and charcoals has been studied in the last years (1,3,6–8). Two different species, Cr(III) and Cr(VI), are present in aqueous solutions; Cr(III) compounds are stable and occur naturally, whilst Cr(VI) occurs only rarely. While Cr(III) is needed in human diet (in a very small amount), Cr(VI) is very dangerous, causing damage to the nose and lungs, and some of their compounds are known carcinogens. Cr(VI) can be formed from Cr(III) under oxidative conditions.

Cr(VI) is a byproduct of steels making, manufacture of pigments, wood preserving, and electroplating. Cr(III) is an ordinary pollutant in wastewaters from tanneries, and is formed by Cr(VI) reduction in the precipitation method of Cr(VI) disposal. The adsorption of Cr(III) on activated carbon is considered as a secondary method to eliminate this cation from wastewaters.

According to Aggarwal et al. (6), and Leyva Ramos et al. (7), at pH values between 2 and 6.4, Cr(III) is present in aqueous solution mostly as $[Cr(H_2O)_5OH]^{2+}$. Cr(III) is adsorbed on carbon between these pH values, with a maximum at pH 5. Cr(VI), seems to be adsorbed as bichromate $HCrO_4^-$; the adsorption is high at pH 6, and at lower pH values Cr(VI) is reduced catalytically to Cr(III) by the carbon surface. Adsorption capacity increases with temperature for both cations (6,8). An increase in electrolyte concentration of the solution produces an increase in the adsorption capacity of Cr(VI) on oxidized carbon,

because the presence of the electrolyte favors the Cr(VI) reduction to Cr(III), changing the species to be adsorbed from an anion to a cation (3).

In this work, wood sawdust obtained from Eucalyptus grandis wood was used as a raw material for the preparation of activated carbons, taking into account the high development of Uruguayan forest industry, and the possibility of using wood wastes to improve industrial benefits (9). Besides, Cr(III) salts are ordinarily used in the Uruguayan tanneries.

In this initial approach, activated carbons were prepared and oxidized, and the adsorption capacity for Cr(III) was measured in aqueous solutions, at constant temperature and without the addition of buffer solution, to eliminate the influence of additional salts (6).

Three different activation methods were used: air and CO_2 gasification of wood char, and direct CO_2 gasification of wood sawdust. After this, activated carbons were oxidized with HNO_3. Characterization of the carbons was done through elemental analysis, N_2 adsorption, and Fourier transform infrared spectroscopy (FT-IR) spectra. Cr(III) adsorption capacity for oxidized carbons was determined from adsorption isotherms at 25°C.

EXPERIMENTAL

Reagents and Apparatus

Eucalyptus grandis sawdust was obtained from wood logs. Wood chips were obtained from logs, and then milled to 0.385–0.75 mm size (Retsch mill type SM 1000). Air was obtained from a compressor and dried by silica filters. Pure N_2, He, and CO_2 (99.995%) were used for adsorption and gasification. $Cr(NO_3)_9{\cdot}H_2O$ (Fluka), and 70% HNO_3 (Sintorgan), analytical grade, were used.

Wood carbonization and CO_2 activation of chars were performed in a horizontal tubular furnace, at 800°C, as was described elsewhere (9–11). The same method was used for air activation (temperature 400°C, holding time 2 hr) and "direct" CO_2 activation of wood sawdust (temperature 800°C, holding time 2 hr).

For activated carbon oxidation, about 5 g of activated carbon was heated in a beaker up to 80°C. After this, 70% of HNO_3 was added slowly until the final ratio of HNO_3 volume to mass of carbon was 5, and the temperature was maintained until dryness (3). The product was washed with distilled water, filtered until reaching pH = 7, and dried at 110°C for 24 hr.

The carbons obtained are named in this work as C, A, D (CO_2, air, and direct activated carbons, respectively) and OC, OA, and OD when oxidized with HNO_3.

Ultimate analysis was carried out with a Carlo Erba, EA 1108 CHNS-O model. N_2 adsorption–desorption isotherms at 77K were obtained from an automatic volumetric equipment, Quantachrome Corp., model Autosorb-1. Samples were outgassed at 80°C for 8 hr. From N_2 isotherms, BET surface area, Dubinin-Raduschkevich (DR) volume, microporosity distribution and volume, by Horvath Kawazoe (HK) method, and mesoporosity distribution, were determined by Pierce method. Mesoporosity volume was determined from the difference between accumulated volume up to 500 Å, by Pierce method (12,13).

For FT-IR spectra, KBr–carbon pellets were made, and a Bomen Hartmann and Braun MB spectrophotometer was used.

For Chromium isotherms determination, 50 mL of Cr(III) solution and 0.1 g of the oxidized carbon (3) were put in several flasks. The flasks were thermostatized at 25.0 ± 0.5°C into a Stuart Scientific SBS30 shaker water bath, at 60 rpm during 72 hr. A blank for each solution, without carbon, was also put besides the samples. For all solutions, the pH was determined (Cole-Parmer digital pH-meter) before and after adsorption, in the presence of carbon. Chromium content of the solutions was obtained with a Perkin–Elmer 380 atomic flame spectrophotometer (λ 357.9 nm, acetylene/air ratio 50/45, intensity lamp 25 mA). Solutions were put through a centrifuge and diluted to 1–15 mg chromium/L before Cr determination was done. $K_2Cr_2O_7$ was used for calibration curve determination.

For all the experiments, two samples were used, and essays were performed in duplicates.

RESULTS AND DISCUSSION

Carbonization and Activation

Eucalyptus wood has a very low ash content (0.3%). After carbonization, the yield is about 20%, an expectable result for biomass carbonization (11). After char activation, yields for the carbons, with respect to initial wood, are 16.3% (A), 14.5% (C), and 13.9% (D); these values are reasonably similar when compared to the porous structure and functional groups present in the corresponding carbons.

Ultimate analysis (Table 1) reveals a decrease in the O percentage after carbonization, which is a consequence of the loss of heteroatoms during wood decomposition. For A and C, the activation effect is clearly different: the percentage of O slightly increases for CO_2 activation, but there is a strong increment for air activation, showing a more pronounced introduction of oxygenated functions in A. Direct activation, on the other hand, does not show an

Table 1. Ultimate Analysis for Carbons and Raw Materials (Dry Basis, Ash Free)

Sample	C (%)	N (%)	H (%)	S (%)	O[a](%)
Wood	47.20	0.10	6.00	0	46.70
Char	90.30	0.10	2.10	0	7.50
A	81.07	0.09	1.23	0	16.95
OA	65.54	0.82	1.71	0	31.92
C	90.88	0.12	0.73	0	8.27
OC	70.54	0.68	1.44	0	27.34
D	93.32	0.20	0.53	0	5.95
OD	68.55	0.89	1.13	0	29.10
OD-Cr	62.97	0.72	1.89	0	34.42[b]

[a] Difference.
[b] O + Cr.

increase in the heteroatom concentration; on the contrary, it presents a lower O concentration than C, and a higher C concentration.

Surface area and porosity for activated carbons were studied. Isotherms (Figs. 1 and 2) are type I with hysteresis (13). The BET surface area and micropore volumes, shown in Table 2, show an increase with respect to char, in the order A < D < C. This increment is in accordance with the inverse of the reactivity of the gas used (9–11). A small presence of mesopores, is detected, more remarkable for D. The DR and HK volumes are almost the same for all the carbons, showing that there is no significant presence of wide micropores.

Carbons FT-IR spectra are shown in Figs. 3 and 4 and assignable peaks in Table 3.

Char FT-IR spectrum shows a very slight developed structure, as functional groups are eliminated mostly during pyrolysis process (14). A peak at 1110 cm^{-1} is attributed to C—O bonds.

For activated carbons a number of peaks are found, detailed as 3460 cm^{-1}: corresponding to partially combinated carboxylic acids O—H stretching. Interaction among O—H groups leads to a broad peak and will shift frequencies to low (3300–2500 cm^{-1}) wave number values (15). On the other hand, nonassociated O—H stretching peaks appear sharply at wave numbers above 3600 cm^{-1}. So, those peaks at 3460 cm^{-1} would represent partially associated O—H functional groups that can interact with some similar neighbor functional groups (explaining peak broadness). As carboxylic acid concentration is low and the groups are more dispersed on the carbon surface, wave number is shifted to higher values than the usually associated ones (16–21). It is not possible to state whether the carboxylic acid functional group stands by itself or it is in

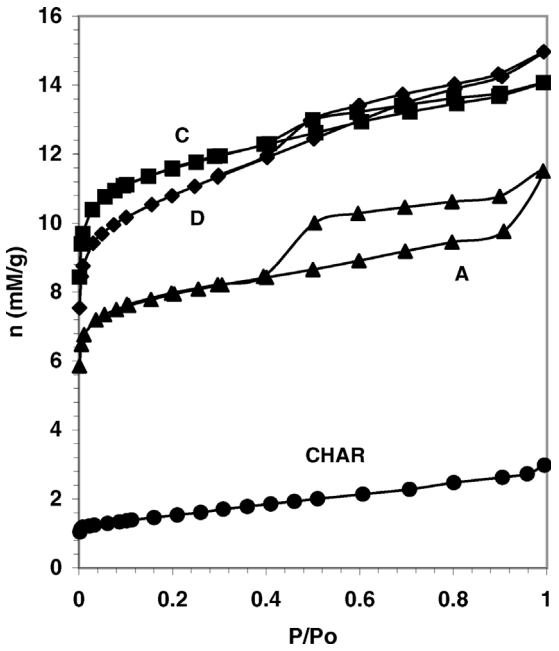

Figure 1. N_2 adsorption–desorption (77K) isotherms of activated carbons and char.

equilibrium with the lactone form. Although bands at 1730–1680 cm^{-1} that confirm this functional group appear in the spectra, they could be overlapped by some other important bands in this region. Further references for these statements are given in the following paragraphs.

2930 and 2855 cm^{-1}: two sharp peaks corresponding to C—H stretching in CH_3 and CH_2 groups. The identification of these groups is confirmed by the presence of another peak at nearly 1450 cm^{-1}, observed in almost all the other spectra.

1700–1800 cm^{-1}: a sharp peak at 1700 cm^{-1}, attributable to cyclic or open ketone, or ester carbonyl, is observed in A; could be present but overlapped in C and D. An ester carbonyl would be accompanied by an important peak in the 1100 cm^{-1} region, that could be overlapped by the lactone C—O stretching peak (16) (see 1100 cm^{-1} region).

1650–1550 cm^{-1}: peaks in this region are assigned to olefinic C═C bond vibrations (22).

1700–1750 cm^{-1} and 1050–1100 cm^{-1}: carbonyl (1700 cm^{-1}) and simple C—O bonds (1100 cm^{-1}) are present. The peak at 1700 cm^{-1}, confirms the presence

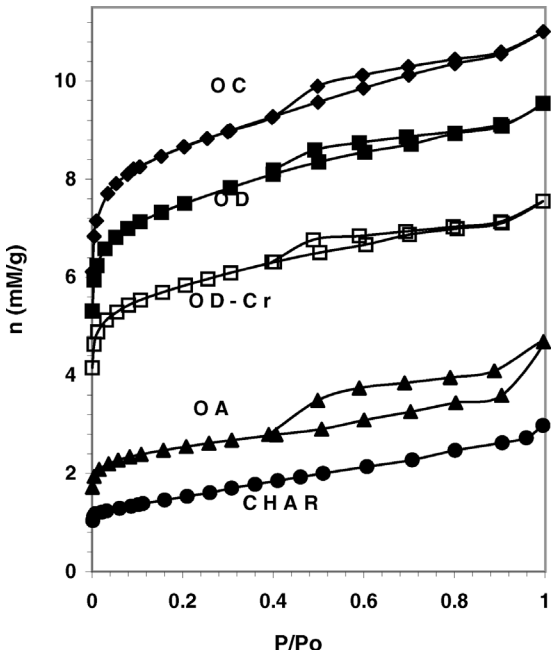

Figure 2. N_2 adsorption–desorption (77K) isotherms of oxidized activated carbons and char.

Table 2. Porosity Parameters for Carbons and Raw Materials, Determined from N_2 Adsorption at 77K

Sample	A_{BET} (m^2/g)	V_{DR} N_2 (cm^3/g)	V_{MICRO} (cm^3/g)	V_{MESO} (cm^3/g)
Char	490	0.21	0.21	0.05
A	680	0.27	0.27	0.04
OA	210	0.08	0.09	0.04
C	1000	0.39	0.39	0.05
OC	740	0.29	0.29	0.05
D	910	0.35	0.37	0.12
OD	550	0.25	0.25	0.05
OD-Cr	490	0.05	0.20	0.04

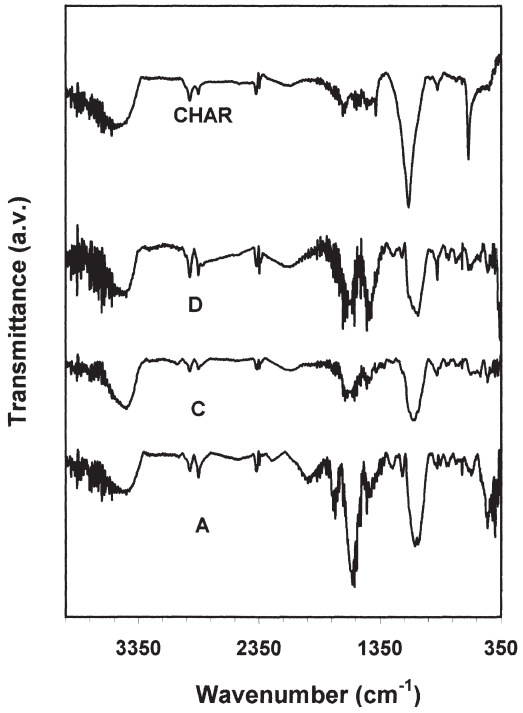

Figure 3. Activated carbons: FT-IR spectra.

of lactone groups that show a characteristic broad peak between 1050 and 1100 cm^{-1} for C—O stretching. The wavenumber, lower than those in normal carbonyls in isolated lactones, is due to lactone ring tension and high conjugation level of the carbon matrix. As an example, high-conjugated lactone molecules as cumarine (see below) present a characteristic sharp peak at 1704 cm^{-1} [(21)].

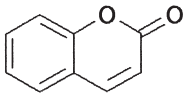

cumarine

As lactones are in equilibrium with the open form (carbonyl-acid) due to the presence of water in wet carbon, the 3460 cm^{-1} peak could also confirm the lactone presence. The influence of the activation method on surface modifications was also studied by comparing the char and activated carbons spectra. For A, there is a clear development and better resolution for carbonyl peaks at 1700 cm^{-1} (lactonized and free ones); this effect is much lower for C, showing D

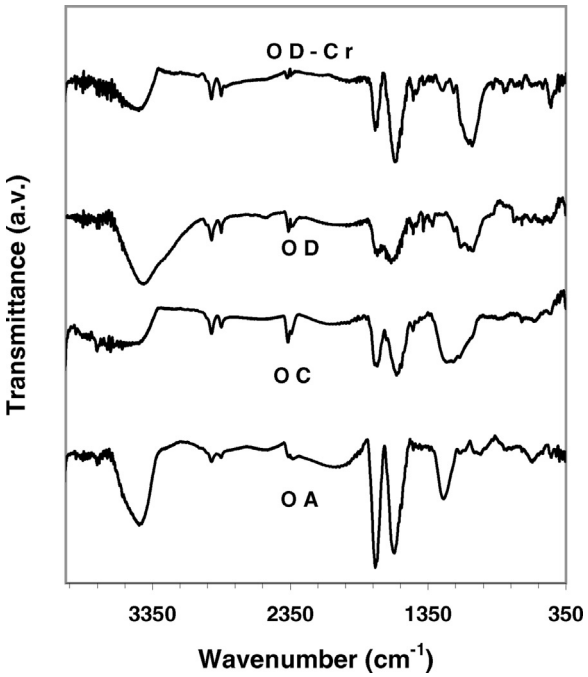

Figure 4. Oxidized activated carbons: FT-IR spectra.

an intermediate effect (22,23). Oxygen in air is responsible for higher oxidation in A, in comparison to CO_2 for C and D. For C, CO_2 had to react with a relatively ordered and less reactive structure (char heated at 800°C during 2 hr) than D, where the pyrolysis is occurring at the same time than the carbon–CO_2 reaction. So, a higher oxidation is to be expected for D than for C (11).

Table 3. FTIR Peaks

Sample	Wavenumber (cm^{-1})
Char	3518, 1112
A	3467, 2931, 2854, 1718, 1577, 1054
OA	3454, 2929, 2862, 1737, 1602, 1247
C	3470, 2931, 2858, 1637, 2560, 1087
OC	3470, 2923, 2854, 1737, 1722, 1538, 1222
D	3469, 2929, 2858, 1795, 1610, 1440, 1056
OD	3450, 2930, 2853, 1734, 1638, 1169, 1123–1040

Nitric Acid Oxidation

After nitric oxidation, the weight increases a little, as a result of introduction of heteroatoms at the carbon surface. This is confirmed in ultimate analysis (Table 1), where the O percentage increases in the sequence OC $<$ OD $<$ OA. For N, the sequence is OC $<$ OA $\cong$ OD.

The HNO_3 oxidation produces a diminution of BET surface area and microporous volume, though N_2 isotherms shapes are maintained (Table 2 and Fig. 1). This effect is explained in terms of micropore blocking, for the presence of big functional groups, or collapse of micropore structure (3). Since the molecular volume of HNO_3 is relatively high, oxidation would be produced on mesopores and wide micropores, blocking N_2 accesibility to the micropores. For mesopore volume, there is not an oxidation effect for C and A oxidation, but porous volume decreases for oxidation of D. It seems as if the N_2 blocking effect for D affects micro and mesoporosity.

For oxidized activated carbons, FT-IR spectra characteristics are similar to unoxidized carbons. However, nitric acid oxidation introduces several changes. Major differences are detailed below.

The 3450–3460 cm^{-1} peak does not change significantly, showing that the functional group or its neighboring is unchanged. In the 1550–1800 cm^{-1} region, the spectra show remarkable changes that could be assigned to adsorbed N—O and C—O structures (24). The 1700 cm^{-1} peak is displaced to 1750 cm^{-1}, revealing a more important presence of lactones. Stretching C—O peak is displaced to higher wavenumbers (1250), so lactone presence could be confirmed. Carbonyl peaks from free carbonyls (1100 cm^{-1}), could be masked in this region.

Other peaks (2930, 2855 cm^{-1}) remain unchanged; these would not be affected by nitric oxidation.

These results are in accordance to the observed O and N increment for oxidized carbons.

Cr(III) Adsorption

For adsorptions, resultant pH is 3–4 (Table 4); the pH value does not change during adsorption. As is established by Leyva Ramos et al. (7), at pH values between 2 and 6.4, Cr(III) is present in aqueous solution as $Cr(OH)^{2+}$. Cr(III) adsorption on carbon is verified between these pH values, too, with a maximum at pH $=$ 5. At the working pH, Cr(III) is therefore adsorbed onto activated carbon.

For isotherms determinations, it was verified that equilibrium is reached with a contact time of 72 hr. Isotherms are shown in Fig. 5; for these, Freundlich

Table 4. pH Variations for Cr(III) Adsorption on Oxidized Carbons

Sample	Initial pH	Equilibrium pH
OA	3.0	2.8
OC	4.0	3.9
OD	3.7	2.8–3.0

model (2,25) fits (Table 5). Adsorption capacity was compared for D and OD. As expected, the unoxidized carbon has a clearly lower capacity (18 mg/g for OD, 2 mg/g for D).

Cr(III) is adsorbed on all the oxidized carbons, the increasing maximum adsorption capacity being OD < OC < OA. The maximum observed capacity for OA is 29 mg/g (Table 6). This higher adsorption capacity for OA is explained in terms of a higher surface concentration of oxygenated groups, as was concluded from FT-IR and elemental analysis.

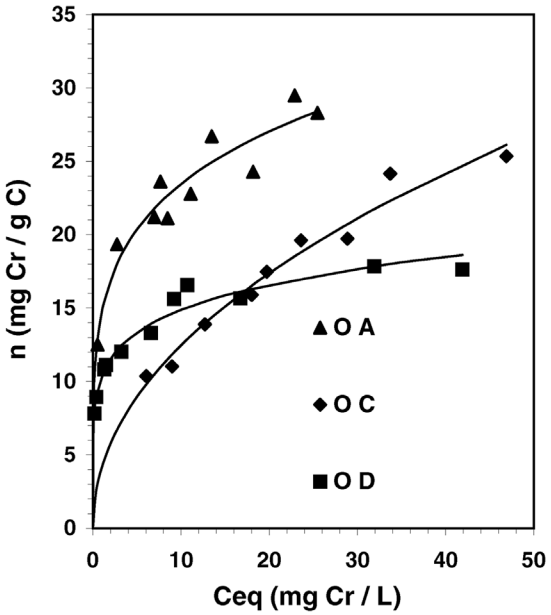

Figure 5. Cr(III) adsorption isotherms and Freundlich fittings.

Table 5. Freundlich Parameters for Cr(III) Adsorption on Oxidized Carbons ($n = kC$), n = mg Cr(III) Adsorbed/g Carbon, C = Equilibrium Concentration, mg Cr(III)/L, k = Freundlich Constant, R^2 = Linear Correlation Coefficient

Sample	k	a	R^2
OA	0.0146	0.20	0.937
OC	0.00414	0.48	0.973
OD	0.0104	0.16	0.973

The adsorption of Cr(III) increases the blocking effect for N_2 adsorption found in oxidized carbons: for OD-Cr, BET surface area and micropore volume decrease in comparison to the original OD (Table 4 and Figs. 1 and 2), so the adsorbed cation is placed at the micropore entry in such a way as to obstruct N_2 passage. The size of hydrated cation could influence too (8).

Surface areas occupied by Cr(III), $S_{Cr(III)}$, were calculated from Cr(III) adsorption capacity by using an aqueous cation diameter of 0.922 nm (26). They are shown in Table 6. For OC and OD, $S_{Cr(III)}$ is lower than A_{BET}, showing that active sites for Cr(III) are lower than N_2 ones, an expected result. On the other hand, for OA, $S_{Cr(III)}$ is higher than A_{BET}. This could be possible if Cr(III) ions could be retained on the surface, where N_2 could not. N_2 adsorption is physicallike, occurring on accessible sites on the surface, hence excluding those sites occupied by functional groups. The Cr^{3+} cation would be adsorbed preferably on sites with a negative charge, so sites with oxygenated groups could retain these ions; adsorption would be pH dependent, as is observed (1). Another possibility is a swelling effect of the porous structure, in the aqueous solution (27).

Cr adsorption does not affect the surface groups present in the oxidized carbon, as can be seen in Fig. 4, where OD and OD-Cr spectra are identical.

Table 6. Surface Areas Occupied by Adsorbed Cr(III) on Oxidized Carbons

Sample	$C_{max.}$ (mg Cr/g C)	$S_{Cr\ (III)}$ (m^2/g)	A_{BET} (m^2/g)
OA	29	290	210
OC	25	251	750
OD	18	181	550

CONCLUSIONS

Cr(III) adsorption capacity of different activated carbons was enhanced by nitric acid oxidation. Oxygenated functions were introduced in the carbon matrix, in the form of carbonyls, carboxyls, lactones, and nitrogenated functions as nitrates or nitrites, as revealed by FT-IR. These groups were responsible for the increment of chromium adsorption capacity. The way by which the activated carbon is prepared influences the type and surface concentration of the functional groups introduced by subsequent oxidation, and it was found that air gasification of wood char produced the higher increment in Cr(III) adsorption capacity.

Reduction of porosity accessibility for nitric oxidation was confirmed, as is stated in the literature, but subsequent Cr(III) adsorption produced an even higher reduction. The low cost of the activating agent and low temperature used, along with wood waste utilization, make air activation an interesting way to produce carbon with improved capacity to retain chromium, which has been an aiding agent for decontamination.

ACKNOWLEDGMENTS

This project had financial support from CSIC, and PEDECIBA. The authors want to thank the Departamento "Estrella Campos", School of Chemistry, for FT-IR, flame spectrophotometry, and ultimate analysis assistance. Special thanks to Quím. Carlos Gastellú and Prof. Eleuterio Umpiérrez for FT-IR spectra interpretation, and to the Departamento Forestal, School of Agronomy, for providing wood samples.

REFERENCES

1. Bansal, R.; Donnet, J.; Stoeckli, F. *Active Carbon*; Marcel Dekker Inc. New York, 1988.
2. Mattson, J.; Mark, H. *Activated Carbon. Surface Chemistry and Adsorption from Solution*; Marcel Dekker, Inc.: New York, 1971; 165.
3. Bautista Toledo, I.; Rivera Utrilla, J.; Ferro García, M.A.; Moreno Castilla, C. Influence of the Oxygen Surface Complexes of Activated Carbons on the Adsorption of Chromium Ions from Aqueous Solutions: Effect of Sodium Chloride and Humic Acid. Carbon **1994**, *32*, 93–100.
4. Marzal, P.; Seco, A.; Gabaldón, C. Cadmium and Zinc Adsorption Onto Activated Carbon: Influence of Temperature, pH and Metal/Carbon Ratio. J. Chem. Tech. Biotechnol. **1996**, *66*, 279–285.

5. Namasivayam, C.; Kadirvelu, K. Uptake of Mercury (II) from Wastewater by Activated Carbon from an Unwanted Agricultural Solid By-Product: Coirpith. Carbon **1999**, *37*, 79–84.
6. Aggarwal, D.; Meenakshi, G.; Bansal, R.C. Adsorption of Chromium by Activated Carbon from Aqueous Solutions. Carbon **1999**, *37*, 1989–1997.
7. Leyva Ramos, R.; Fuentes Rubio, L.; Guerrero Coronado, R.; Mendoza Barron, J. Adsorption of Trivalent Chromium from Aqueous Solutions onto Activated Carbon. J. Chem. Tech. Biotech. **1995**, *62*, 64–67.
8. Jayson, G.; Sangster, J.; Thompson, G.; Wilkinson, M.y. Adsorption of Chromium from Aqueous Solutions onto Activated Carbon Cloth. Carbon **1993**, *31* (3), 487–492.
9. Tancredi, N.; Cordero, T.; Rodríguez Mirasol, J.; Rodríguez, J.J. Activated Carbons from Eucalyptus Wood. Influence of the Carbonization Temperature. Sep. Sci. Technol. **1997**, *32* (6), 1115–1126.
10. Tancredi, N.; Cordero, T. Activated Carbon from Uruguayan Eucalyptus Wood. Fuel **1996**, *75* (15), 1701–1706.
11. Tancredi, N. *Preparación y Caracterización de Carbón Activado a Partir de Madera de Eucalipto* Ph.D. Thesis, Facultad de Química, Universidad de la República, Uruguay.
12. Sing, K.S.W.; Gregg, S.J. *Adsorption, Surface Area and Porosity*, 2nd Ed.; Academic Press: London, 1982.
13. Rouquerol, F.; Rouquerol, J.; Sing, K. *Adsorption by Powders and Porous Solids*; Academic Press: London, 1999.
14. Ibarra, J.V.; Moliner, R.; Bonet, A.J. FT-IR Investigation on Char Formation During the Early Stages of Coal Pyrolysis. Fuel **1994**, *73* (6), 918–924.
15. Silverstein, R.M.; Bosser, G.C.; Morril, T.C. *Spectrometric Identification of Organic Compounds*, 5th Ed; John Wiley and Sons Inc.: New York, 1991; 117–120.
16. Figueiredo, J.L.; Pereira, M.F.R.; Freitas, M.M.A.; Órfao, J.J.M. Modification of the Surface Chemistry of Activated Carbons. Carbon **1999**, *37*, 1379–1389.
17. Pradham, B.K.; Sandle, N.K. Effect of Different Oxidizing Agent Treatments on the Surface Properties of Activated Carbons. Carbon **1999**, *37*, 1323–1332.
18. Vinke, P.; Van der Euk, M.; Verbree, M.; Voskamp, A.F.; Van Bekkum, H. Modification of the Surfaces of a Gas-Activated Carbon and a Chemically Activated Carbon with Nitric Acid, Hypochlorite, and Ammonia. Carbon **1994**, *32* (4), 675–686.
19. Corapciouglu, M.O.; Huang, C.P. The Surface Acidity and Characterization of Some Commercial Activated Carbons. Carbon **1987**, *25* (4), 569–578.

20. Hesse, M.; Meier, H.; Zeen, B. *Spektroskopisce Methoden in der Organischen Chemie*; Georg Tiheme Verlag: Stuttgart, 1995; Chap. 1.
21. Pouchert, J.M. *Aldrich Library FT-IR Spectra*, 1st Ed.; Aldrich Chemical Company Inc.: USA, 1985; Vol. II, 632.
22. Gómez Serrano, V.; Piriz-Almeida, F.; Durán-Valle, C.J.; Pastor-Villegas, J. Formation of Oxygen Structures by Air Activation. A Study by FT-IR Spectroscopy. Carbon **1999**, *37*, 1528–1571.
23. Gómez Serrano, V.; Acedo Ramos, M.; López Peinado, J.; Valenzuela Calahorro, C. Oxidation of Activated Carbon by Hydrogen Peroxide. Study of Surface Functional Groups by FT-IR. Fuel **1994**, *73* (3), 387–395.
24. Gómez Serrano, V.; Acedo Ramos, M.; López Peinado, J.; Valenzuela Calahorro, C. Mass and Surface Changes of Activated Carbon Treated with Nitric Acid. Thermal Behaviour of the Samples. Thermochim. Acta **1997**, *291*, 109–115.
25. Warhurst, A.; McConnachie, G.; Pollard, J. Characterisation and Applications of Activated Carbon Produced from Moringa Oleifera Seed Husks by Single-Step Steam Pyrolysis. Carbon **1997**, *31* (4), 761.
26. Nightingale, E.R., Jr. Phenomenological Theory of Ion Solvation. Effective Radii of Hydrated Ions. J. Phys. Chem. **1959**, *63*, 1381–1387.
27. Nandi, S.P.; Walker, P.L., Jr. Adsorption of Dyes from Aqueous Solution by Coals, Chars, and Active Carbons. Fuel **1971**, *50*, 345–366.

Received February 2001